WOOD RESEARCH
64 (1): 2019
83-96

DEGRADATION OF WOOD FIRE RETARDANT BY UV-ASSISTED BIOMIMETIC OXIDATION OVER Cu([H_4]SALEN) USING BDE209 AS A MODEL

Xujie Lu
Hainan Tropical Ocean University, School of Ecology and Environment
Sanya, China

Wuhan Textile University, Hubei Key Laboratory of Biomass Fibers and Eco-Dyeing and Finishing
Wuhan, China

Yong-Gui Li
Minjiang University, Fujian Key Laboratory of Novel Functional Textile Fibers and Materials
Fuzhou, China

Xue-Fei Zhou
Wuhan Textile University, Hubei Key Laboratory of Biomass Fibers and Eco-Dyeing and Finishing
Wuhan, China

Nankai University, Key Laboratory of Advanced Energy Materials Chemistry of Ministry of Education of China
Tianjin, China

Minjiang University, Fujian Key Laboratory of Novel Functional Textile Fibers and Materials
Fuzhou, China

Kunming University of Science and Technology. Faculty of Chemical Engineering
Kunming, China

Guangxi University For Nationalities, Guangxi Key Laboratory of Chemistry and Engineering of Forest Products
Nanning, China

Fu-Hou Lei, Zu-Guang Liu, Ting Wang
Guangxi University for Nationalities, Guangxi Key Laboratory of Chemistry and Engineering of Forest Products
Nanning, China

(Received July 2018)

ABSTRACT

This work aimed to study mineralization and detoxification of BDE209 by biomimetic oxidation. The removal rate (RR) of BDE209 of process was comparatively investigated in the presence of UV radiation using immobilized Cu([H_4]salen) complexes (Cu([H_4]salen)/IM and Cu([H_4]salen)/SB) as biomimetic catalysts. Their neat and [H_2]salen complexes were compared towards BDE209 degradation. UV effects were evaluated according to RR. Ecotoxicities were measured for treated BDE209 solutions and explained in terms of total organic carbon (TOC). The results showed that UV-Cu([H_4]salen)/SB process evidently gave high RR and low ecotoxicity in BDE209 degradation, indicating a significant superiority of biomimetic catalysis, complex reduction and immobilization and UV radiation.

KEYWORDS: Biomimetic catalysis, BDE209, UV radiation, mineralization, detoxification.

INTRODUCTION

Wood consumption is tremendous in China, the annual consumption is nearly a 500 million m^3, including logs, wood-based panels, etc. (Yun et al. 2017). Wood is widely used in the fields of furniture, interior decoration and architecture because of its high strength-weight ratio, rich texture, beautiful tone, excellent environmental characteristics and easy processing. At the same time, because wood is a flammable biomass material, it is often treated by adding various fire retardants to reduce the flammability or delay the combustion (Yeniocak et al. 2016, Cong et al. 2018).

Polybrominated biphenyl ethers (PBDEs), as a class of brominated flame retardants, have been widely used in various consumer products because of their excellent flame-retardant performance. However, as PBDEs are frequently detected in samples, they are becoming a rising concern worldwide due to their toxicity and recalcitrance in the environment (Ren et al. 2018). Consequently, efforts are substantially undertaken at international level to debrominate PBDEs, such as physical (Huang et al. 2013), biological (Man et al. 2015), chemical oxidation (Shi et al. 2015), chemical reduction and photolysis method (Lei et al. 2018). However, the common drawback of these processes is the high treatment cost. Therefore, the best strategy seems to be the combination of biological processes and chemical oxidation (Klauson et al. 2015).

Biomimetic catalysts offer feasible alternatives to degrade POPs (persistent organic pollutants) as they mimic enzymes in terms of catalytic behaviour, suggesting that POPs might be treated by chemical oxidation following the mechanism of biocatalysis (Zhang et al. 2018). Ge et al. (2017) provided a new strategy in designing various metal phthalocyanine catalysts for degradation of chlorophenol pollutants. Chen et al. (2017) reported that the destruction efficiency of 4-chlorophenol increased remarkably with the combined photocatalysis and biomimetic catalysis using imidazole (IMD)-functionalized modification of g-C3N4 and axial coordination with hemin. Another interesting study of organic pollutant degradation using biomimetic catalyst was reported by Gazi et al. (2010). They presented [Fe(III)-salen]Cl complex as catalyst for the degradation of organic dyes, indicating that biomimetic catalysis is a promising technique to treat POPs. Moreover, salen complex was also used in the catalytic degradation of chlorophenols (2-CP, 3-CP and 4-CP) (Wang et al. 2015), and the addition axial imidazole drastically improved the catalytic efficiency on the catalytic oxidation of pentachlorophenol by changing its protonation state (Christoforidis et al. 2016). Meng et al. (2017) successfully intercalated M(salen) (M=Co or

Ni) into ZnCr layered double hydroxides (LDHs) through coprecipitation method and the results showed that M(salen)-intercalated ZnCr-LDHs exhibited significantly higher catalytic activities than the traditional LDHs on the RhB degradation.

Simultaneously, it was previously found by our group that biomimetic catalysis showed high reaction selectivity and efficiency relatively as compared with conventional processes, especially for immobilized and/or reduced biomimetic catalysts (Tang and Zhou 2015, Zhou 2015, Zhou and Tang 2016). In fact, tetrahydro-salen ([H_4]salen) complexes displayed a high activity compared to their schiff-base counterparts due to the flexible C-N bonds in complexes by the hydrogenation of C=N (Das et al. 2013, Liu et al. 2015). The immobilized complexes showed a higher activity than the neat complexes (Kianfar et al. 2018), indicating a promising pathway for complete debromination of decabromodiphenyl ether over Cu([H_4]salen).

Therefore, the methodology was extended to the treatment of decabromodiphenyl ether (BDE209) in this work for improving the mineralization and detoxification. However, because of the difficulty in degradation of BDE209 in oxidation, UV radiation was designed to enhance the biomimetic catalysis. Currently, little researches reported in literatures with regard to UV assisted biomimetic oxidation for persistent organic pollutants (POPs). Although BDE209 releases toxic substances in use, it is still frequently used as fire retardant in the field of wood-based materials, especially in developing countries. Therefore, this study is about significance to provide a new oxidative process for detoxification of wood fire retardant BDE209 against environment.

MATERIALS AND METHODS

Materials

BDE209 (99.99%) was obtained from AccuStandard. Solvents (Sigma-Aldrich, HPLC grade) were stored at 4°C. All other chemicals (Sinopharm Chemical Reagent Co., Ltd, analytical grade) were commercially available and were used as received. All glass wares were washed using detergent in an ultrasonic bath and rinsed with deionized water, acetone and n-hexane prior to use.

Preparation of catalyst

Neat and immobilized Cu[H_4]salen and their [H_2]salen counterparts have been prepared and characterized by our group as published in our literature, and their textural characteristics were listed in Tab. 1 (Zhou 2014).

Tab. 1: Characteristics of neat and encapsulated Cu(II)[H_4]salen and [H_2]salen complexes.

Catalyst	Cu content (wt %)	SBET ($m^2 \cdot g^{-1}$)	VBJH ($cm^3 \cdot g^{-1}$)	DBET (nm)
NaY	-	584.38	0.32	3.22
Cu([H_2]salen)	19.00	-	-	-
Cu([H_2]salen)/IM	1.88	270.10	0.15	2.17
Cu([H_2]salen)/SB	1.21	581.77	0.26	2.22
Cu([H_4]salen)	19.22	-	-	-
Cu([H_4]salen)/IM	3.99	308.38	0.17	2.21
Cu([H_4]salen)/SB	0.86	528.03	0.28	2.28

IM - impregnation method; SB - ship-in-a-bottle method; specific surface area - SBET ($m^2 \cdot g^{-1}$); pore volume - VBJH ($cm^3 \cdot g^{-1}$); pore diameter - DBET (nm).

Catalytic trials

Catalytic trials were performed under strictly exclusion of sunlight in a UV reactor (Fig. 1). pH value was adjusted with buffer solution. pH 2: phosphoric acid+sodiun hydroxide; pH 3: citric acid+sodium citrate; pH 4: potassium biphthalate; pH 6: acetic acid+sodium acetate; pH 7: sodium dihydrogen phosphate+dibasic sodium phosphate; pH 8: dipotassium hydrogenphosphate+potassium phosphate monobasic; pH 9: Tris+hydrochloric acid; pH 11: sodium bicarbonate+sodiun hydroxide). The mixture was injected into nitrogen for 30 min to remove the dissolved oxygen in the reaction system prior to the experiment. Deionized water was used in all experiments.

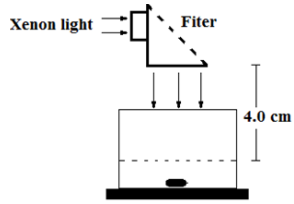

Fig. 1: Schematic diagram of UV reactor.

The mixtures were sampled at convenient times, and were added with methanol and catalase successively for terminating free radical reactions. The samples were filtered with 0.22 μm disk filter for the next analyses.

Determination of Br- concentration

The concentration of bromide ion was analyzed quantitatively by a DIONEX IC-2000 ion chromatograph (IC) equipped with a conductivity detector based on a linear calibration which was established by using standards of known ion concentrations. The separation of ions was performed on a 4×250 mm column (IonPac AS11-HC, P/N51786), with mobile phase flow of 1 mL·min^{-1}. The mobile phase was 1.00 mM $NaHCO_3$ and 3.00 mM Na_2CO_3. Therefore, based on Br- concentration, removal rate (RR, %) was defined for BDE209 as follows:

$$RR\,(\%) = \frac{[Br^-]_t / 80}{[BDE209]_0 / 959.17 \times 10} \times 100 \quad (1)$$

where: $[Br^-]^t$ - represents the concentration of bromide ion (mg·L^{-1}) at t of reaction time,
$[BDE209]_0$ - represents the initial concentration of BDE209 (mg·L^{-1}).

Determination of BDE209 concentration

The samples were analyzed at 240 nm by HPLC (Dionex P680-UVD 170U). Separation was achieved on an Eclipse Plus C18 column (150 mm×4.6 mm×5 μm). The mobile phase was 30:1 v/v acetonitrile: water, which was degassed before use. Quantitation was achieved using standard curves.

Determination of TOC

Total organic carbon (TOC) of the solutions obtained from the treatments was determined on a TOC VWP Analyzer (Shimadzu) using wet oxidation.

Ecotoxicity measurement

Ecotoxicities of the solutions resulting from these treatments were measured following the Microtox Acute Toxicity Test with Microtox Model 500 Toxicity Analyzer using a freeze-dried

preparation of marine bacterium *Vibrio fischeri* (*Photobacterium phosphoreum*) (Thongrom et al. 2014).

RESULTS AND DISCUSSION

Catalyst effect on BDE209 removal

RR was comparatively explored in BDE209 degradation for catalyst optimization. As shown in Fig. 2, the reduction and immobilization of the complexes were generally considered to be important in the improvement of catalytic efficiency (Jin et al. 2012). For example, the catalytic performance of Cu([H_4]salen) was much better than that of corresponding complex both in unimmobilized and immobilized types according to the RR (Fig. 2). At reaction of 30 min, Cu([H_4]salen) yielded 54.7% BDE209 degradation, but Cu([H_2]salen) exhibited a low BDE209 removal (33.8 %). Additionally, a very low BDE209 conversion (< 2.0%) was obtained in control trials in the absence of UV radiation and catalyst, as shown in Fig. 2.

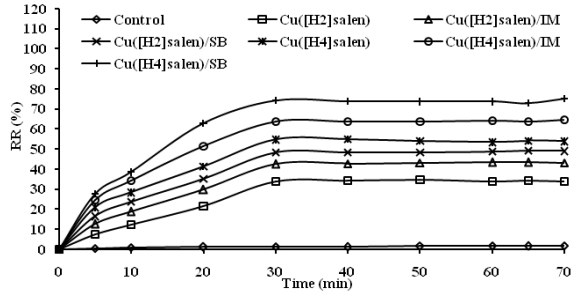

Fig. 2: Catalyst effect on BDE209 removal. [BDE209]=40 mg·L^{-1}; [catalyst]=0.80 g ·L^{-1}; [H_2O_2]=40 µmol·L^{-1}; pH=7.0; UV intensity=2.0 W·m^{-2}.

On the other hand, among these catalysts, Cu([H_4]salen)/SB yielded the highest removal value of BDE209 (0-74.2%), which reflected the synergistic effect of reduction and immobilization on Cu([H_2]salen). Comparatively, when Cu([H_4]salen)/IM, Cu([H_2]salen)/SB and Cu([H_2]salen)/IM were employed in catalytic degradation, BDE209 conversion was 0-63.8%, 0-48.3% and 0-42.4%, respectively (Fig. 2). This was consistent with a decrease in micro pore diameter from 2.28 nm to 2.17 nm (Tab. 1) and this can be explained as changing the packing mode of the salen complexes with improvement in flexibility by hydrogenation on C=N and stability by immobilization, decreasing the formation of dimeric-, oxo- and peroxo-bridged species in complexes which deactivated easily (Subramaniam et al. 2016). Moreover, the other essential factor that generated improvement by SB-catalysts was due to the fact that micro pores were not easy to be blocked and active species were not easy to be lost from the super cages during immobilizing complex in NaY by SB-method as compared to IM-method (Fan et al. 2016).

pH Effect on BDE209 removal

Cu([H_4]salen)/SB was chosen as a catalyst for further optimizing reaction conditions. Fig. 3 shows the effects of pH on the BDE209 degradation at pH value of 2-11 when the concentration of Cu([H_4]salen)/SB was 0.80 g·L^{-1}. As shown in Fig. 3, the RR increased as pH values increased. When pH increased from 2 to 8, RR increased from 64.8% to 78.8%. Meanwhile, pH value above

8 was actually too alkaline for BDE209 degradation. These results suggest that adding NaOH is beneficial to improve the BDE209 degradation.

Both OH– and Na+ in aqueous solution may promote the decomposition of BDE209 by reaction with acidic species (e.g. CH_3COOH) and Br– derived from by-products in BDE209 degradation. Moreover, Na_2CO_3 may act as a catalyst in aromatic ring-opening step (Shih and Tai 2010).

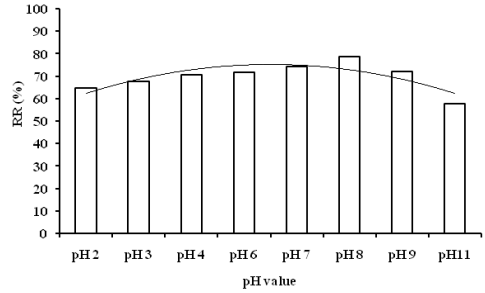

Fig. 3: pH effect on BDE209 removal. [BDE209]=40 mg·L^{-1}; [Cu([H$_4$]salen)/SB]=0.80 g·L^{-1}; [H$_2$O$_2$]=40 μmol·L^{-1}; 30 min; UV intensity=2.0 W·m^{-2}.

In addition, oxygen species of salen complex influence the reaction severity depending on the equilibrium between binuclear and mononuclear oxo-complexes. The mononuclear oxo-complexes are more favourable for enhancing reactivity than the binuclear oxo-complexes in the equilibrium solution of salen oxygen adducts, whereas the equilibrium can be shifted towards the more catalytically active mononuclear oxo-complexes by tuning the reaction conditions, such as reacting in weak alkaline medium (Sandaroos et al. 2010). NaOH offers hydroxide anion as axial ligand in favour of coordination of salen with oxygen forming mononuclear oxo-complexes (Bogaerts et al. 2015). In our early study, it was also found that addition of NaOH to biomimetic system reduced the generation of intermediate binuclear oxo-complexes, and accelerated the abstraction of phenolic-H atoms by mononuclear species (Zhou 2014).

Concentration effect of hydrogen peroxide on BDE209 removal

Fig. 4 shows the effects of the concentration of hydrogen peroxide on the degradation of BDE209 at pH 8, when the concentration of hydrogen peroxide in solution ranged from 0 μmol·L^{-1} - 40 μmol·L^{-1}. As shown in Fig. 4, RR increased dramatically in the presence of hydrogen peroxide, indicating a significant oxidation effect between hydrogen peroxide and BDE209. Particularly, RR increased from 3.3% to 78.2% at 30 min, after adding hydrogen peroxide in a concentration range of 0 μmol·L^{-1} - 30 μmol·L^{-1} in solution. After that, RR were barely changed even the concentration of hydrogen peroxide increased from 30 μmol·L^{-1} to 40 μmol·L^{-1}.

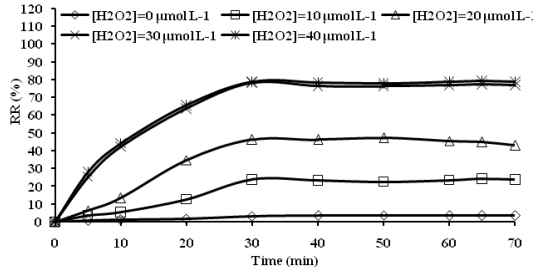

Fig. 4: Concentration effect of hydrogen peroxide on BDE209 removal. [BDE209]=40 mg·L^{-1}; [Cu([H$_4$] salen)/SB]=0.80 g·L^{-1}; pH=8; UV intensity=2.0 W·m^{-2}.

Hydrogen peroxide follows a free radical reaction mechanism and generates free radicals such as L-Cu-O-O• (L=ligand) by aerobic oxidation of Cu([H$_4$]salen). From previous research on free radical reaction of salen complex, the tind (induction time) of hydrogen peroxide in biomimetic catalysis ranges from 0.2 s to 0.4 s (Shimazaki and Yamauchi 2011, Kurahashi and Fujii 2013). Thus, the free radical reaction of hydrogen peroxide takes place in a short time; in other words, adding hydrogen peroxide to solution increases the quantity of L-Cu-O-O•, which in turn promotes the conversion of BDE209 in solution. This is similar to the results reported by Lu and Zhou (2014). They suggested that hydrogen peroxide accelerated the cleavage of ether bond because hydrogen peroxide oxidized and generated reactive L-M-O-O• rapidly.

Concentration effect of catalyst on BDE209 removal

Concentration effect of Cu([H$_4$]salen)/SB on the BDE209 removal was comparatively discussed, and the results were shown in Fig. 5. RR of BDE209 evidently increased with the increase of Cu([H$_4$]salen)/SB concentration in a concentration range of 0 g·L^{-1} - 0.60 g·L^{-1}. It was found in this work that for BDE209 degradation, little improvements were observed when Cu([H$_4$]salen)/SB concentration was more than 0.60 g·L^{-1} and the best RR was 77.8% at 30 min under the concentration of 0.60 g·L^{-1} Cu([H$_4$]salen)/SB. On this condition, RR of BDE209 in catalytic degradation was about ten times of that in absence of Cu([H$_4$]salen)/SB.

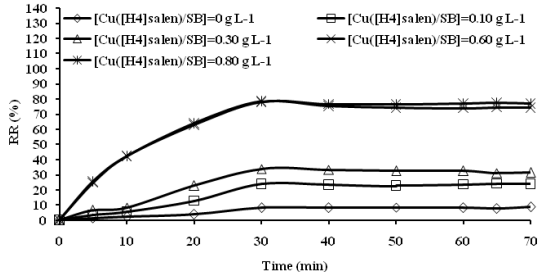

Fig. 5: Concentration effect of Cu([H$_4$]salen)/SB on BDE209 removal. [BDE209]=40 mg·L^{-1}; [H$_2$O$_2$]=30 μmol·L^{-1}; pH=8; UV intensity=2.0 W·m^{-2}.

Initial concentration effect of substrate on BDE209 removal

Since, substrate concentrations have been reported to be important for degradation (Qin et al. 2017), the effects of BDE209 concentration of 20-80 mg·L^{-1} on RR by the present oxidation were examined and the results are shown in Fig. 6. The results did reveal the substrate concentration

dependence. At concentrations higher than 40 mg·L^{-1}, RR decreased rapidly due to the high concentration of substrate (Fig. 6a), but a positive relationship of BDE209 concentration and removal quantity (RQ) was also observed, as shown in Fig. 6b. However, consequently, the concentration of 40 mg·L^{-1} BDE209 was fixed, which was optimal for degradation of BDE209.

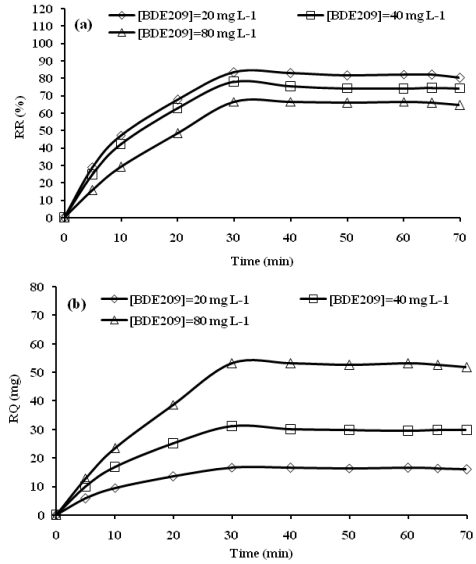

Fig. 6: Initial concentration effect of substrate on BDE209 removal. [Cu([H$_4$]salen)/SB]=0.60 g·L^{-1}; [H$_2$O$_2$]=30 μmol·L^{-1}; pH=8; UV intensity=2.0 W·m^{-2}.

UV intensity effect on BDE209 removal

Six varieties of UV irradiations (2 W·m^{-2}, 4 W·m^{-2}, 6 W·m^{-2}, 8 W·m^{-2}, 10 W·m^{-2} and 12 W·m^{-2}) were employed to evaluate the UV effect on RR at 0.60 g·L^{-1} [Cu([H$_4$]salen)/SB], 30 μmol·L^{-1} H$_2$O$_2$ and 30 min when the reaction medium was set to be pH 8. These results were compared to a control test without UV irradiation and the effects of irradiations on RR are shown in Fig. 7.

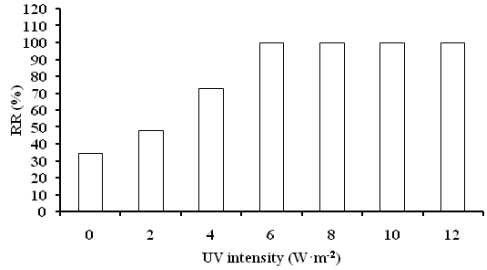

Fig. 7: UV intensity effect on BDE209 removal. [BDE209]=40 mg·L^{-1}; [Cu([H$_4$]salen)/SB]=0.60 g·L^{-1}; [H$_2$O$_2$]=30 μmol·L^{-1}; pH=8; time 30 min.

The UV irradiations highly improved RR in BDE209 treatment, compared with the non-UV reaction. Especially, the UV irradiation of 6.0 $W \cdot m^{-2}$ displayed the highest acceleration effect compared with other UV intensities, and the corresponding RR was 100 %. Although we did not carry out the other experiments using polybrominated diphenyl ethers (PBDEs) as substrates at the same conditions, it can be expected that the combination of UV irradiation and biomimetic catalysis will exhibit superiority in PBDEs decomposition, relatively, due to the promotion of catalytic activity by UV irradiation. Jose et al. (2017) presented that oxygen species including L-M-O-O• and other active oxygen radicals can easily arise through the absorption of UV by salen complex compared to other materials in aerobic oxidation. UV irradiation may also increased the amount of acetic acid in intermediate products, which promoted the formation of a Cu(III)-phenoxyl radical complex (L-Cu-O-O•) resulting the further degradation of intermediate products derived from BDE209 (Vinck et al. 2010) as shown in Fig. 8.

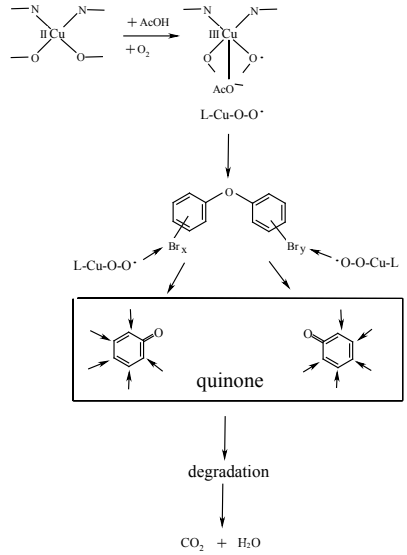

Fig. 8: Formation of a Cu(III)-phenoxyl radical complex promoted by acetic acid resulting the further degradation of intermediate products derived from BDE209.

Quinone intermediates, serving as electron shuttles, could play an important catalytic role in the oxidation of BDE209, which promoted the decomposition of intermediates, resulting in the mineralization of BDE209 (Chen and Pignatello 1997, Zhou et al. 2017). This was consistent with the results obtained by some researches towards chlorophenols (Zhou et al. 2011, Lin et al. 2012, Van et al. 2017).

Ecotoxicity of treated-solutions

Tab. 2 shows the values of BDE209 degradation, TOC conversion and ecotoxicity obtained upon UV assisted biomimetic oxidation using different catalysts.

Tab. 2: Effect of catalytic treatment on ecotoxicity of treated-solutions.

Catalysis	RR (%)	TOC conversion (%)	Ecotoxicity (T.U.)
Untreated solution	0	0	58.5
Cu([H_2]salen)	66.8	57.3	20.4
Cu([H_2]salen)/IM	72.5	61.3	14.3
Cu([H_2]salen)/SB	78.2	66.8	11.7
Cu([H_4]salen)	84.3	69.2	8.3
Cu([H_4]salen)/IM	89.4	71.4	5.4
Cu([H_4]salen)/SB	100	76.7	1.06

[BDE209]=40 mg·L^{-1}; [catalyst]=0.60 g·L^{-1}; [H_2O_2]=30 μmol·L^{-1}; pH=8; UV intensity= 6.0 W·m^{-2}.

Ecotoxicities of the six treated solutions were lower than the control, but all the treated solutions were more toxic than the deionized water. The solution with a lowest ecotoxicity was the resulting from treatment with Cu([H_4]salen)/SB since complete BDE209 degradation was achieved allowing a higher TOC conversion representative of considerable mineralization. However, it should be stated that the residual H_2O_2 (2.6 μmol·L^{-1}) did not significantly lead to an increase in solution toxicity in terms of the meaningful decline of ecotoxicity although it was toxic.

CONCLUSIONS

Biomimetic catalysis makes full use of high efficiency and high selectivity in reaction chemically and enzymatically, respectively. As a complex derived from the reduction and immobilization of Cu([H_2]salen), Cu([H_4]salen)/SB showed a superiority in terms of removal and ecotoxicity of BDE209 undergoing UV radiation. Meanwhile, increasing catalyst concentration, H_2O_2 concentration, UV intensity and reaction pH evidently enhanced the degradation of BDE209. Considering mineralization and detoxification, the optimal reaction conditions were obtained, from which the removal rate of BDE209 was 100 %, and its ecotoxicity of Cu([H_4] salen)/SB-treated solution was 1.06 T.U. It can be concluded that immobilized M([H_4]salen) complexes (M=metal) were most likely to successfully treat PBDEs.

ACKNOWLEDGEMENTS

This work was supported by the National Natural Science Foundation of China (21766015), the Open Research Foundation of Hubei Key Laboratory of Biomass Fibers and Eco-dyeing and Finishing of Wuhan Textile University (STRZ2018002), the Open Research Foundation of Key Laboratory of Advanced Energy Materials Chemistry of Ministry of Education of China of Nankai University (111 project B12015), the Open Research Foundation of Fujian Key Laboratory of Novel Functional Textile Fibers and Materials of Minjiang University (FKLTFM1819), the Scientific Research and Trial-Production Project of Sanya (2017KS07), and the Open Research Foundation of Guangxi Key Laboratory of Chemistry and Engineering of Forest Products of Guangxi University for Nationalities (GXFC17-18-03).

REFERENCES

1. Bogaerts, T., Wouters, S., Voort, P.V.D., Speybroeck, V.V., 2015: Mechanistic investigation on oxygen transfer with the manganese - salen complex. ChemCatChem 7(17): 2711-2719.
2. Chen, J., Pignatello, J., 1997: Role of quinone intermediates as electron shuttles in Fenton and photo assisted Fenton oxidations of aromatic compounds. Environmental Science and Technology 31(8): 2399-2406.
3. Chen, X., Lu, W., Xu, T., Li, N., Qin, D., Zhu, Z., Wang, G., Chen, W., 2017: A bio-inspired strategy to enhance the photocatalytic performance of g-C3N4 under solar irradiation by axial coordination with hemin. Applied Catalysis B: Environmental 201: 518-526.
4. Christoforidis, K.C., Pantazis, D.A., Bonilla, L.L., Bletsa, E., Louloudi, M., Deligiannakis, Y., 2016: Axial ligand effect on the catalytic activity of biomimetic Fe-porphyrin catalyst: An experimental and DFT study. Journal of Catalysis 344: 768-777.
5. Cong, J.Y., Yang, G.C., Zhao, L.J., Zhang, Q.H., 2018: The synergistic smoke suppression effect of ferric oxide on flame retardant wood-polyurethane composites. Wood Research 63(2): 305-320.
6. Das, A., Kureshy, R.I., Prathap, K.J., Choudhary, M.K., Rao, G.V.S., Khan, N.U.H., Abdi, S.H.R., Bajaj, H.C., 2013: Chiral recyclable Cu(II)-catalysts in nitroaldol reaction of aldehydes with various nitroalkanes and its application in the synthesis of a valuable drug (R)-isoproterenol. Applied Catalysis A-General 459: 97-105.
7. Fan, F., Fan, W., Li, R., 2003: Fe-containing Y as a host for the preparation of a ship-in-a-bottle catalyst. Journal of Molecular Catalysis A: Chemical 201(1-2): 137-144.
8. Gazi, S., Ananthakrishnan, R., Singh, N.D.P., 2010: Photodegradation of organic dyes in the presence of [Fe(III)-salen]Cl complex and H_2O_2 under visible light irradiation. Journal of Hazardous Materials 183(1-3): 894-901.
9. Ge, S.X., Li, D.P., Xu, J.L., Sun, G.F., Fa, W.J., Zhang, M., Tan, J.S., Huang, J., Du, Q.S., 2017: Insight into the reactivity difference of two iron phthalocyanine catalysts in chromogenic reaction: DFT theoretical study. Inorganic and Nano-Metal Chemistry 47(10): 1406-1411.
10. Huang, K., Lin, K., Guo, J., Zhou, X., Wang, J., Zhao, J., Zhou, P., Xu, F., Liu, L., Zhang, W., 2013: Polybrominated diphenyl ethers in birds from Chongming Island, Yangtze estuary, China: Insight into migratory behavior. Chemosphere 91: 1416-1425.
11. Jin, C., Fan, W., Jia, Y., Fan, B., Ma, J., Li, R., 2012: Encapsulation of Cu[H_4]Salpn in zeolite Y and its catalytic properties for the oxidation of cycloalkanes. British Journal of Haematology 89(4): 698-703.
12. Jose, T.J., Simi, A., Raju, M.D., Praveen, P.L., 2017: Estimation of high and low UV intensity profiles of mesogenic oxovanadium (IV) salen complexes: Doubling effect of homologue number. Molecular Crystals and Liquid Crystals 650(1): 46-55.
13. Kianfar, A.H., Tavanapour, S., Eskandari, K., Azarian, M.H., Mahmood, W.A.K., Bagheri, M., 2018: Experimental and theoretical structural determination, spectroscopy and electrochemistry of cobalt (III) Schiff base complexes: immobilization of complexes onto Montmorillonite-K10 nanoclay. Journal of the Iranian Chemical Society 15(2): 369-380.
14. Klauson, D., Kivi, A., Kattel, E., Klein, K., Viisimaa, M., Bolobajev, J., Velling, S., Goi, A., Tenno, T., Trapido, M., 2015: Combined processes for wastewater purification: treatment of a typical landfill leachate with a combination of chemical and biological oxidation processes. Journal of Chemical Technology and Biotechnology 90(8): 1527-1536.

15. Kurahashi, T., Fujii, H., 2013: Unique ligand-radical character of an activated cobalt salen catalyst that is generated by aerobic oxidation of a cobalt(II) salen complex. Inorganic Chemistry 52(7): 3908-3919.
16. Lei, M., Wang, N., Guo, S., Zhu, L.H., Ding, Y.B., Tang, H.Q., 2018: A one-pot consecutive photocatalytic reduction and oxidation system for complete debromination of tetrabromodiphenyl ether. Chemical Engineering Journal 345: 586-593.
17. Lin, Z., Chen, H., Zhou, Y., Ogawa, N., Lin, J.M., 2012: Self-catalytic degradation of ortho-chlorophenol with Fenton's reagent studied by chemiluminescence. Journal of Environmental Sciences 24(3): 550-557.
18. Liu, B., Chai, J., Feng, S.S., Yang, B.S., 2015: Structure, photochemistry and magnetic properties of tetrahydrogenated Schiff base chromium(III) complexes. Spectrochimica Acta Part A - Molecular and Biomolecular Spectroscopy 140: 437-443.
19. Lu, X.-J., Zhou, X.-F., 2014: Co(salen)-catalysed oxidation of synthetic lignin-like polymer: H_2O_2 effects. Oxidation Communications 37(2): 572-582.
20. Man, Y.B., Chow, K.L., Man, M., Lam, J.C.W., Lau, F.T.K., Fung, W.C., Wong, M.H., 2015: Profiles and removal efficiency of polybrominated diphenyl ethers by two different types of sewage treatment work in Hong Kong. Science of the Total Environment 505: 261-268.
21. Qin, Y., Han, B., Cao, Y., Wang, T., 2017: Impact of substrate concentration on anammox-UBF reactors start-up. Bioresource Technology 239: 422-429.
22. Ren, X., Zeng, G., Tang, L., Wang, J., Wan, J., Liu, Y., Yu, J., Yi, H., Ye, S., Deng, R., 2018: Sorption, transport and biodegradation - An insight into bioavailability of persistent organic pollutants in soil. Science of the Total Environment 610-611: 1154-1163.
23. Sandaroos, R., Goldani, M.T., Damavandi, S., Mohammadi, A., 2012: Efficient asymmetric Baeyer–Villiger oxidation of prochiral cyclobutanones using new polymer-supported and unsupported chiral Co(salen) complexes. Journal of Chemical Sciences 124(4): 871-876.
24. Shi, J., Qu, R., Feng, M., Wang, X., Wang, L., Yang, S., Wang, Z., 2015: Oxidative degradation of decabromodiphenyl ether (BDE 209) by potassium permanganate: Reaction pathways, kinetics, and mechanisms assisted by density functional theory calculations. Environmental Science and Technology 49(7): 4209-4217.
25. Shih, Y.H., Tai, Y.T., 2010: Reaction of decabrominated diphenyl ether by zero valent iron nanoparticles. Chemosphere 78(10): 1200-1206.
26. Shimazaki, Y., Yamauchi, O., 2011: Recent Advances in metal-phenoxyl radical chemistry. Indian Journal of Chemistry 50A: 383-394.
27. Subramaniam, P., Anbarasan, S., Devi, S.S., Ramdass, A., 2016: Modulation of catalytic activity by ligand oxides in the sulfoxidation of phenylmercaptoacetic acids by oxo(salen) chromium(V) complexes. Polyhedron 119: 14-22.
28. Tang, K., Zhou, X.-F., 2015: Co(salen) catalysed oxidation of synthetic lignin-like polymer: Pyridine effects. Theoretical Foundations of Chemical Engineering 49(6): 877-883.
29. Thongrom, B., Amornpitoksuk, P., Suwanboon, S., Baltrusaitis, J., 2014: Photocatalytic degradation of dye by Ag/ZnO prepared by reduction of Tollen's reagent and the ecotoxicity of degraded products. Korean Journal of Chemical Engineering 31(4): 587-592.
30. Van, A.P., Van, den B.R., Degreve, J., Dewil, R., 2017: A pilot-scale coupling of ozonation and biodegradation of 2,4-dichlorophenol-containing wastewater: The effect of biomass acclimation towards chlorophenol and intermediate ozonation products. Journal of Cleaner Production 161: 1432-1441.

31. Vinck, E., Murphy, D.M., Falli, I.A., Strevens, R.R., Doorslaer, S.V., 2010: Formation of a Cobalt(III)-phenoxyl radical complex by acetic acid promoted aerobic oxidation of a Co(II) salen complex. Inorganic Chemistry 49(5): 2083-2092.
32. Wang, H.H., Yang, J., Liu, Y.Y., Song, S.Y., Ma, J.F., 2015: Heterotrimetallic organic framework assembled with Fe-III/Ba-II/Na-I and schiff base: Structure and visible photocatalytic degradation of chlorophenols. Crystal Growth and Design 15(10): 4986-4992.
33. Yeniocak, M., Colak, M., Goktas, O., Koca, I., 2016: Fire resistance performance of wood materials coloured with eco-friendly pomegranate skin (Punica granatum) extracts. Wood Research 61(3): 363-372.
34. Yun, H., Li, K.F., Hu, C.S., Tu, D.Y., 2017: Adsorption and fixation of soluble fire retardancy in *Populus russkh* and *Cunninghamia lanceolata*. Wood Reseach 62(2): 253-260.
35. Zhang, Q., Chen, S., Wang, H., Yu, H., 2018: Exquisite enzyme - Fenton biomimetic catalysts for hydroxyl radical production by mimicking an enzyme cascade. ACS Applied Materials and Interfaces 10(10): 8666-8675.
36. Zhou, S., Gu, C., Qian, Z., Xu, J., Xia, C., 2011: The activity and selectivity of catalytic peroxide oxidation of chlorophenols over Cu-Al hydrotalcite/clay composite. Journal of Colloid and Interface Science 357: 447-452.
37. Zhou, Y., Jiang, J., Gao, Y., Pang, S.Y., Yang, Y., Ma, J., Gu, J., Li, J., Wang, Z., Wang, L.H., 2017: Activation of peroxymonosulfate by phenols: Important role of quinine intermediates and involvement of singlet oxygen. Water Research 125: 209-218.
38. Zhou, X.-F., 2014: Application of zeolite-encapsulated Cu(II) [H_4]salen derived from [H_2] salen in oxidative delignification of pulp. RSC Advances 4(53): 28029-28035.
39. Zhou, X.-F., 2015: Catalytic oxidation and conversion of kraft lignin into phenolic products using zeolite-encapsulated Cu(II)[H_4]salen and [H_2]salen complexes. Environmental Progress and Sustainable Energy 34(4): 1120-1128.
40. Zhou, X.-F., Tang, K., 2016: Combining laccase with Cu(salen) catalysts for oxidation of kraft lignin. Drewno 59(198): 35-47.
41. Zhou, X.-F., 2014: Co(salen) catalysed oxidation of synthetic lignin-like polymer: NaOH effects. Polish Journal of Chemical Technology 16(3): 93-98.

Yong-Gui Li
Fujian Key Laboratory of Novel Functional Textile Fibers and Materials
Minjiang University
No.200, Xiyuangong Road
Minhou, 350108
Fuzhou
China
Corresponding author: lygwxjd@sina.com